3-16-2023

Identification of Gap Junction Genes Involved in the Tail-Flip Escape Circuit of Marbled Crayfish

Rajit S. Roy
Illinois State University, rsroy@ilstu.edu

IDENTIFICATION OF GAP JUNCTION GENES INVOLVED IN THE TAIL-FLIP ESCAPE CIRCUIT OF MARBLED CRAYFISH

RAJIT SHEKHAR ROY

47 Pages

Escape responses are highly stereotyped behaviors that enable organisms to avoid threats in their environment. To ensure the rapid and robust execution of these behaviors, they are often mediated by dedicated neuronal circuits with fast feed-forward signal propagation. Rectifying electrical synapses, which allow electrical current to preferentially flow only in one direction, are a hallmark of such circuits, and facilitate rapid and stereotyped neuronal signaling for fast, reflexive behaviors. *In vitro* studies have suggested that it is the heterotypic distribution of the gap junction proteins (called innexins in invertebrates), i.e., possessing different innexins in pre- and postsynaptic neurons, that enables the rectification of the electrical synapse. However, the presence of distinct pre- and postsynaptic gap junction proteins and the functional roles of these proteins have not been established in escape circuits. I am using the tail-flip escape behavior of crayfish, a classical behavioral model for understanding escape responses, to study gap junction proteins. The neuronal circuitry of the crayfish tail-flip behavior has been largely worked out, with specialized giant neurons identified for the two major types of escape modes in the animal – the lateral giant (LG) and medial giant (MG) tail-flip. In both MG and LG escape circuits, rectifying electrical synapses facilitate rapid signal transmission from primary afferents to the motor neurons. However, the innexin proteins expressed in the crayfish nervous system and

contributing to these rectifying synapses are unknown. To address this gap in knowledge, I used the marbled crayfish *(Procambarus virginalis),* the only crayfish species with identified genome and transcriptome. Employing bioinformatics, I identified five putative innexin genes (named Inx1 - Inx5), four of which were expressed in the nervous system and likely contribute to tail flip escape responses. Four of the five putative innexins (Inx2 – 5) were expressed in the ventral nerve cord and three of them (Inx2, 3 and 5) were also expressed in the brain. To test the contribution of these innexins to the escape behavior, I used RNA interference to reduce innexin expression. This was followed by behavioral assays to test whether MG and LG tail flips were altered by the RNAi treatment. My results indicate that reduction in expression of two of the five identified innexins, i.e., Inx2 and Inx3, using RNAi resulted in a significant delay in the onset of the LG tail-flip. This suggests that these two innexin proteins contribute to the formation of gap junction channels in the LG tail-flip circuit. In contrast, no significant effect was found for the MG tail-flip following the same RNAi approach. From these results, I conclude that there are four innexin proteins that are expressed in marbled crayfish nervous system and are homologous to other invertebrate innexins. Moreover, marbled crayfish innexin 2 and 3 constitute the gap junction channels that form electrical synapses in the LG tail-flip circuit and are important for robust signal transmission.

KEYWORDS: Electrical synapses, Giant neurons, Gap junctions, Innexins, Escape response, Tail-flip, RNA interference

IDENTIFICATION OF GAP JUNCTION GENES INVOLVED IN THE TAIL-FLIP ESCAPE CIRCUIT OF MARBLED CRAYFISH

RAJIT SHEKHAR ROY

A Thesis Submitted in Partial
Fulfillment of the Requirements
for the Degree of

MASTER OF SCIENCE

School of Biological Sciences

ILLINOIS STATE UNIVERSITY

2023

IDENTIFICATION OF GAP JUNCTION GENES INVOLVED IN THE TAIL-FLIP ESCAPE CIRCUIT OF MARBLED CRAYFISH

RAJIT SHEKHAR ROY

COMMITTEE MEMBERS:

Wolfgang Stein, Chair

Andres Vidal-Gadea, Co-Chair

Martin Engelke

ACKNOWLEDGMENTS

I express my deepest gratitude to Dr. Wolfgang Stein and Dr. Andres Vidal-Gadea for offering me the opportunity to conduct research in their labs. I also thank Dr. Martin Engelke for agreeing to be on my thesis committee and for his valuable suggestions and insights about my project. In addition, I shall remain indebted to Abbi Benson, MS for setting up the groundwork for my research through her own preliminary experiments and results on the topic. Furthermore, I am grateful to all my former and current lab members for their persistent support and encouragement inside and outside the lab. Last but not the least, I would take this opportunity to acknowledge the contribution of undergraduate researchers in the Stein and Vidal-Gadea labs, especially Jennifer Miller and Caleb Hudspath, for assisting me with some of the experiments discussed hereafter.

R.S.R

CONTENTS

TABLES

FIGURES

CHAPTER I: INTRODUCTION

Escape responses are among the best studied behaviors with well-characterized neuronal circuits in many different species. Because of their rapid execution and rather simple connectivity, the neuronal circuits underlying escape reflexes have been studied intensively. A particular emphasis has been on the mechanisms of fast neuronal signal propagation, allowing animals to avoid predators and noxious stimuli in their environment. Most escape responses are highly stereotyped behaviors that occur with short latency after stimulus detection. Well-studied examples include the C-start startle in zebrafish, the giant fiber escape in Drosophila, the escape jump in locusts, and the tail-flip escape reflex of crayfish. In all cases, latencies are extremely short – e.g., 3-10 ms for the zebrafish C-start startle reflex, 20-30 ms for the locust escape jump [Tabor et al, 2014; Santer et al, 2008], <7 ms for the Drosophila escape [von Reyn, et al., 2017], and less than 30 ms for crayfish [Edwards, 2017]. Such rapid reflex behaviors are enabled by dedicated neuronal circuits with minimalistic feedforward circuit structure that involve only 1-2 synapses between sensory neurons and the muscles that execute the escape reflex. These circuits often involve electrical synapses, which enable fast signal processing with minimal delay.

Unlike chemical synapses which involve the movement of neurotransmitters across a synaptic cleft, electrical synapses form a physical connection between adjacent neurons (called gap junction) that enable the flow of electrical current between them. Electrical synapses can be classified into two major types – rectifying and non-rectifying. Rectifying electrical synapses allow current to flow only in one preferred direction while non-rectifying synapses allow bidirectional flow [Marder 1998; Furshpan and Potter, 1959; Giaume, Kado, and Korm, 1987].

Because of their electrical properties, non-rectifying synapses are prevalent in networks of neurons where they mediate the synchronization of whole cell populations [Marder and Calabrese, 1996; Rela and Szczupak, 2004]. Rectifying synapses, on the other hand, are often found in circuits that mediate fast, reflexive behaviors since they facilitate feedforward information flow from the pre- to postsynaptic neurons [Auerbach and Bennett, 1969; Furshpan and Potter, 1959]. The properties of rectification appear to be similar in vertebrate and invertebrate gap junctions, even though the underlying gap junction proteins belong to separate protein families, namely connexins and innexins respectively.

In-vitro studies have suggested that rectification may result from the structural properties of gap junction channels [Phelan et al., 2008]. Homotypic gap junctions are formed from identical gap junction proteins on either side of the synapses [Fig. 1]. It has been suggested that this kind of structure leads to non-rectifying synapses which allow bidirectional current flow. Heterotypic synapses, on the other hand, are formed from different gap junction proteins present on either side of the synapse which may result in rectification with unidirectional current flow. Nonetheless, the evidence for the structural composition of rectifying electrical synapses only comes from *in vitro* experiments involving functional expression of Drosophila innexins in Xenopus oocytes [Phelan et al, 2008]. Based on the results of these experiments, the proposed structure of rectifying and non-rectifying gap junction channels and the distribution of proteins in such channels is shown in Fig. 1. However, direct evidence that heterotypic synapses underlie rectification in escape circuits is amiss, and the specific role of distinct gap junction proteins in escape responses remains poorly understood.

I am using the neuronal circuits underlying crayfish tail-flip escape responses to study gap junction proteins. Electrical synapses, rectification and their involvement in escape responses were first identified in this circuit [Furshpan and Potter, 1959]. Electrical synapses contribute to two different types of tail flips – the LG (lateral giant) and the MG (medial giant) tail flip [Edwards et al, 1999]. The LG tail flip is elicited by a mechanical stimulus to the tail of the animal and is mediated by the LG neuron. The mechanosensory afferents and the LG neuron are connected via rectifying electrical synapse. LG then excites the giant motor neurons (MoGs) through another rectifying synapse [Edwards et al, 1999]. The MG tail flip, on the other hand, is elicited by mechanosensory stimuli to the head of the animal and is mediated by the MG neuron. MG then excites the MoGs via a rectifying electrical synapse [Edwards, 2017]. The non-giant (NG) tail flip is another type of tail flip which is stimulated by slow stimuli and does not involve the giant command neurons [Edwards et al, 1999]. Thus, the behavioral and neural characteristics of crayfish tail flip escape is well-understood. However, the molecular composition of its underlying neural circuitry is yet to be fully discerned. Specifically, the gap junction proteins that constitute the electrical synapses in the giant neuron escape circuits are unknown.

My thesis addresses the question which innexins contribute to the LG and MG crayfish tail-flip responses. Since LG and MG escape circuits employ rectifying electrical synapses and rectification appears to require heterotypic gap junctions [Phelan et al., 2008], I hypothesized that multiple innexins, which share homology with other known innexin proteins, are expressed in the crayfish nervous system, and that several of them contribute to the tail flip.

Figure 1

Proposed composition of gap junction channels connecting two adjacent neurons.

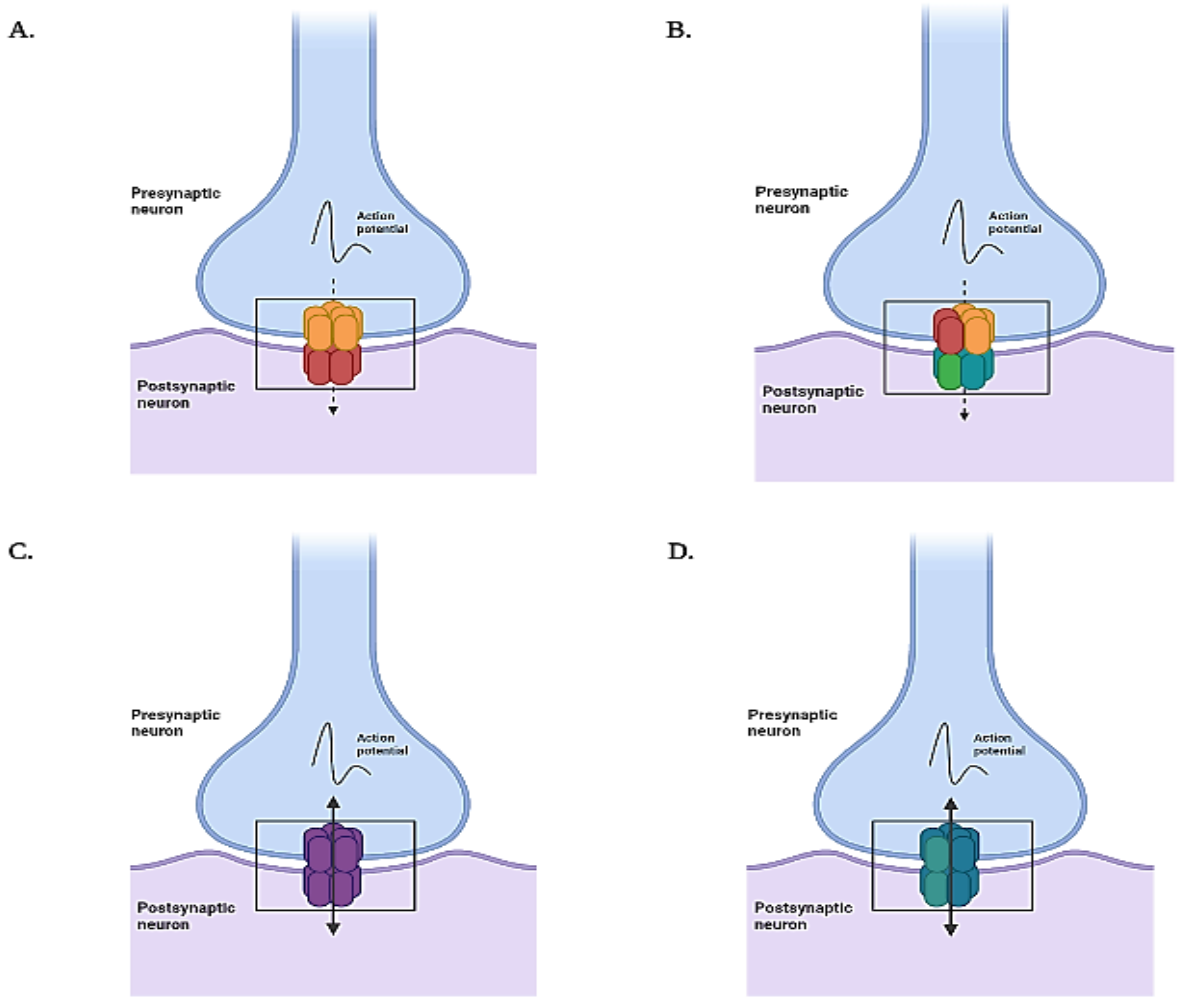

In vitro experiments in Xenopus oocytes indicate that rectifying electrical synapses can be formed by heterotypic channels (asymmetric distribution of gap junction proteins). A, B: The proposed options for synaptic assembly of pre- and postsynaptic innexin proteins for heterotypic rectifying synapses. C, D: Non-rectifying synapses are proposed to be built by homotypic channels (symmetric distribution of proteins). The figures show the proposed options for synaptic assembly of pre- and postsynaptic innexin proteins.

Image created with BioRender.com. Each color represents a unique protein.

CHAPTER II: EXPERIMENTAL APPROACH

I. Identification of neuronal innexins in marbled crayfish

Genome and transcriptome sequence analysis

To identify putative gap junction proteins, I searched the *Procambarus virginalis* genome sequence assembly available in NCBI (https://www.ncbi.nlm.nih.gov/data-hub/genome/?taxon=2065263) for innexin sequences. Specifically, I searched for homologs of the 8 known innexin sequences from Drosophila. The Drosophila sequences were downloaded from NCBI as FASTA files and used for homology search in the crayfish genome using BLASTn. The top blast hit for each fly innexin (max score > 50 and e-value close to 0.0) were used for further analysis.

To identify the transcript regions for the homologous scaffold sequences, I used the locally available marbled crayfish transcriptome sequence and performed a string search against each scaffold in a text editor. The matching transcript region for each scaffold sequence was recorded and numbered as Inx1-5 in their order of identification [Table 1].

Conserved domain search on putative innexins

I used NCBI's Conserved Domain Database (CDD) to identify the conserved domains on marbled crayfish innexin sequences. The transcript sequence of each crayfish innexin was used as query in the CDD search bar to obtain the corresponding domain hits.

Designing primers for innexin sequences in marbled crayfish

To test for expression of putative innexins in marbled crayfish, I designed intron-spanning primers as described by Abbi Benson [Abbi Benson, 2020]. Some of the existing primers available in the lab were also used for expression measurements. Primers were designed in Primer3Plus (version 3.2.6) using the scaffold sequences that corresponded to each crayfish innexin. Several different combinations of forward and reverse primers for the specific innexin sequence were used to select the most effective primer pair. A temperature gradient PCR was set up to estimate the best annealing temperature. Within the constraints of practically feasible primer properties like melting temperature and amplicon size, all effort was made to use the entire scaffold sequence as template for primer design. Furthermore, the Oligo Calc online tool was used to exclude possible hairpins and primer-dimer formations before primer synthesis [Kibbe WA, OligoCalc: an online oligonucleotide properties calculator, 2007].

Crayfish dissection and tissue extraction

Individual marbled crayfish were anesthetized on ice for about 10-15 mins before the dissection. Dissection of individual crayfish was carried out under a stereomicroscope [Leica MZ6, Leica Biosystems, Wetzlar, Germany] while the animal was kept immersed in crayfish saline in a dish. The whole ventral nerve cord and brain tissue were extracted and stored separately in 1.5 ml tubes in either 1-1.5 ml ethanol (for genomic DNA extraction) or 5 volumes of RNA later solution [Thermofisher Scientific, Waltham, MA] by mass (for RNA extraction). The tubes were kept in -30^0C freezer until used.

Genomic DNA extraction

Genomic DNA extraction was performed using the commercially available DNeasy Blood & Tissue Kit [Qiagen, Hilden, Germany]. Crayfish dissection and tissue extraction was done as described above. I used between 20-25 mg of crayfish tissue for extracting genomic DNA using this method to ensure optimal DNA concentration for downstream applications. Tissue (brain and ventral nerve cord) was crushed in 1.5 ml tube using a disposable pestle [RNase-Free Disposable Pellet Pestles, Fisherbrand] to aid in cell lysis. Cell lysis, column binding, wash, and elution steps were performed as described in the kit's manual. The concentration of final eluted DNA was measured using a nanodrop machine [NanoDrop One, ThermoFisher Scientific]. DNA was stored in -20^{0}C in 1.5 ml tubes for future use.

RNA extraction

RNA extraction was performed using the commercially available Direct-zol RNA Miniprep Kit [Zymo Research, Irvine, CA]. As stated above, tissue (20-25 mg) dissected for RNA extraction was stored in RNA later until used. The tissue was removed from RNA later solution and allowed to dry before the extraction steps were carried out. The dried tissue was placed in a new 1.5 ml tube and frozen in dry ice for 10-15 mins. The frozen tissue was crushed using a sterile pestle before adding 300 µl Trizol reagent. The mix was homogenized by pipetting up and down. All other steps were performed in the recommended order as described in the kit method. An additional DNase I treatment was carried out to remove genomic DNA contamination. The extracted RNA was immediately frozen in -30^{0}C overnight in a 1.5 ml tube or converted to complementary DNA (cDNA).

Reverse transcription/cDNA synthesis

To synthesize cDNA from mRNA, I used a commercially available reverse transcription kit [QuantiTect Reverse Transcription Kit, Qiagen]. 1 µg of extracted RNA was used as template for reverse transcription reaction as described in the kit method, which involves two major steps – genomic DNA wipeout (which removes genomic DNA contamination) and reverse transcription (which reverse-transcribes cDNA from mRNA). The synthesized cDNA was quantified using a nanodrop machine and stored in -20^0C until used.

Polymerase Chain Reaction (PCR)

PCR was performed using a commercially available PCR master mix [Phusion Flash High-Fidelity PCR Master Mix, ThermoFisher Scientific] which contains Phusion Flash II DNA Polymerase along with all other reagents needed for PCR, except template and primers. Both genomic DNA and cDNA were used as templates in the PCR reactions as needed. Primers for different innexin sequences were used to amplify innexin genes.

For a 20 µl reaction, the following composition of reaction mixture was used:

Phusion Flash PCR Master Mix: 10 µl

Template DNA: 1 µl

Forward Primer: 1 µl

Reverse Primer: 1 µl

Autoclaved Water: 7 µl

The PCR reaction was set up in a thermocycler [MiniAmp Plus Thermal Cycler, Applied Biosystems, Waltham, MA] with the reaction mix prepared in microcentrifuge tubes and placed in individual heating blocks. The following temperature cycles were used in the PCR reaction:

Initial denaturation: 98^0C – 10 s

Denaturation: 98^0C – 1 s

Annealing: variable temperature based on the primer used – 5 s

Extension: 72^0C – 15 sec/kb of product

Final extension: 72^0C – 1 min

Hold: 4^0C

The annealing temperature for different primer pairs was calculated using the online Tm calculator tool from ThermoFisher Scientific (https://www.thermofisher.com/us/en/home/brands/thermo-scientific/molecular-biology/molecular-biology-learning-center/molecular-biology-resource-library/thermo-scientific-web-tools/tm-calculator.html) using the manufacturer's recommendations for the master mix used. To optimize the annealing temperature for a given primer pair, a temperature gradient PCR was set up to identify the most robust annealing temperature.

Agarose Gel Electrophoresis

I used agarose gel electrophoresis to visualize DNA bands on a gel after PCR amplification. For making 50 ml of 1% agarose gel, 0.5 g of agarose powder was mixed with 50 ml of 0.5% TAE buffer in a 250 ml conical flask. The mixture was then heated in a microwave for 1-2

minutes to dissolve the agar. 2.5 µl of Ethidium Bromide (EtBr), which acts as an intercalating dye, was added to the agar mix after cooling. The volumes stated above were scaled up for making larger gels, i.e., 1 g agar in 100 ml buffer for making 100 ml of 1% gel and 5 µl EtBr. The mixture was then poured onto a gel tray and a plastic comb was placed on one end of the tray to create DNA loading wells. The gel was allowed to solidify for 20-30 minutes before loading DNA into the wells. The gel tray was filled with TAE buffer until all the wells were fully immersed prior to loading DNA. For loading, I used a 5:1 ratio of DNA to loading dye (5 µl DNA + 1 µl loading dye). A DNA ladder was also loaded alongside the DNA samples for size comparison. The positive electrode was connected to the end opposite to the loading wells while negative electrode was connected to the end closest to the wells on the gel tray. The electrophoresis chamber was connected to a power source and allowed to run for about half an hour at 85 V. DNA, being negatively charged, migrates towards the positive electrode and away from the negative electrode based on its mass and thus DNA of different sizes can be separated on a gel.

After the gel run was complete, the agarose gel was carefully removed from the tray and transferred to a gel imager for visualization and imaging [UVP ChemStudio Plus, Analytik Jena, Jena, Germany].

II. Identification of innexins involved in the crayfish escape circuit

Synthesis of double stranded RNA for innexin silencing

For synthesizing double stranded RNA (dsRNA) to induce RNAi silencing of innexin genes, I used a commercially available RNAi kit [MEGAscript RNAi kit, ThermoFisher Scientific]. Marbled crayfish Inx3, Inx4, and Inx5 sequences were used as templates for a high-yield transcription reaction which resulted in the generation of complementary RNA transcripts. The two RNA strands were then hybridized to form a double-stranded RNA for each innexin gene targeted. Finally, dsRNA was purified following nuclease digestion of DNA and single stranded RNA and removal of other contaminants. The purified dsRNA was quantified using a nanodrop machine and run on 1% agarose gel after diluting it 10 times with nuclease-free water [Fig. 2]. To avoid repeated freezing and thawing of dsRNA when used for experiments, I pipetted the dsRNA into 5 µl aliquots in microcentrifuge tubes and stored in -80^{o}C freezer until used. dsRNA against Drosophila *Dmyd* gene was used as control [Abbi Benson, 2020].

dsRNA injection into crayfish

To induce RNAi, I injected dsRNA corresponding to the innexin genes into juvenile crayfish with an average weight of 0.2 g at a working concentration of 3 µg/g of animal weight. The dsRNA was diluted with crayfish saline and injected into the animal using a 50 µl syringe. The injection site was located between the cephalothorax and the abdomen in between two adjacent carapace plates. To avoid excess body fluid volume after injection, an equal volume of hemolymph was removed from the animal before injecting the dsRNA.

Recording and analysis of tail-flip behavior

The tail-flip behavior assay was performed 48 hrs after RNAi injection, as established by previous work in the lab [Abbi Benson, 2020]. To stimulate the MG and LG tail-flips, I used a rectangular animal cage made of plexiglass which was fitted with a pulley mechanism attached to a metallic probe [Fig. 3]. For the MG tail-flip, the animal was stimulated at the head using the metallic probe. For the LG tail-flip, the animal was stimulated on the abdomen. To record the tail-flip behavior, I used a high-speed video camera [Yi Action Camera, Bellevue, WA, USA, 240 frames per second]. The tail-flip videos were analyzed in Tracker software from Open-source physics. Several different behavioral parameters were measured for both the LG and MG tail-flip to analyze the kinetics of escape response, especially latency of flexion onset (for both LG and MG tail-flip), distance traveled on x axis (for MG tail-flip), tail-flip height (for LG tail-flip), and time to peak velocity (for both LG and MG tail-flip). Moreover, the velocity of the metallic probe after release was analyzed in Tracker to ensure that the strength of the mechanosensory stimulus on the animal remained consistent.

The tested animals were sacrificed and dissected to extract RNA from the ventral nerve cord as previously described. The extracted RNA was converted to cDNA as per the previously described protocol to be used for gene expression measurement.

Statistical analyses

Preliminary statistical analysis was performed in Microsoft Excel, including calculation of mean, standard deviation, and standard error for experimental datasets. The p-value for significance testing between pre- and post-treatment data was estimated using paired t-test with 1-tailed distribution. A p-value ≤ 0.05 was considered significant. The assumption of normality

for paired t-test was tested for difference values in the paired behavioral data (pre- vs post-treatment) using SPSS [SPSS Inc., Chicago, IL, USA].

Table 1

Scaffold and transcript identifiers for the 5 innexin sequences in marbled crayfish.

Innexin Name	**Scaffold #**	**Transcript #**
Innexin 1	Scaffold 25651	TR 19635
Innexin 2	Scaffold 25651	TR 16976
Innexin 3	Scaffold 20327	TR 20134
Innexin 4	Scaffold 11516	TR 17309
Innexin 5	Scaffold 3284	TR 6064

Genome assembly database: https://www.ncbi.nlm.nih.gov/assembly/GCA_002838885.1/

Table 2

List of primers used.

Primer Name	**Sequence**	**Purpose**
Innexin 1 Forward	GCAACAAGCACGAGATCAAA	PCR
Innexin 1 Reverse	CGCCAGCATCTTGAGCTTTC	PCR
Innexin 2 Forward	GCCAGATTGGTGACTGGTTT	PCR
Innexin 2 Reverse	CATGCCACACAGGTAACAGG	PCR
Innexin 3 Forward	TTGGTCCTTCGGGTACTTTG	PCR
Innexin 3 Reverse	TCCATGTCCTCCAACATTCA	PCR
Innexin 4 Forward	GACTCGTGGGGACTCAACAT	PCR
Innexin 4 Reverse	CTTCCATCTGGGATCCTGAA	PCR
Innexin 5 Forward	GTTGAAGGGGTATGCCTGAA	PCR
Innexin 5 Reverse	CGCATTGGTCGTTGTTACAC	PCR

(Table continues)

(Table continued)

Primer Name	**Sequence**	**Purpose**
T7 Innexin 2 Forward	TAATACGACTCACTATAGGG AGAGCCAGATTGGTGACTGGTTT	dsRNA synthesis
T7 Innexin 2 Reverse	TAATACGACTCACTATAGGG AGACATGCCACACAGGTAACAGG	dsRNA synthesis
T7 Innexin 3 Forward	TAATACGACTCACTATAGGG AGATTGGTCCTTCGGGTACTTTG	dsRNA synthesis
T7 Innexin 3 Reverse	TAATACGACTCACTATAGGG AGATCCATGTCCTCCAACATTCA	dsRNA synthesis
T7 Innexin 4 Forward	TAATACGACTCACTATAGGG AGAGACTCGTGGGGACTCAACAT	dsRNA synthesis
T7 Innexin 4 Reverse	TAATACGACTCACTATAGGG AGACTTCCATCTGGGATCCTGAA	dsRNA synthesis
T7 Innexin 5 Forward	TAATACGACTCACTATAGGG AGAGTTGAAGGGGTATGCCTGAA	dsRNA synthesis
T7 Innexin 5 Reverse	TAATACGACTCACTATAGGG AGACGCATTGGTCGTTGTTACAC	dsRNA synthesis

Figure 2

Gel image of innexin dsRNA synthesized using MEGAscript RNAi kit.

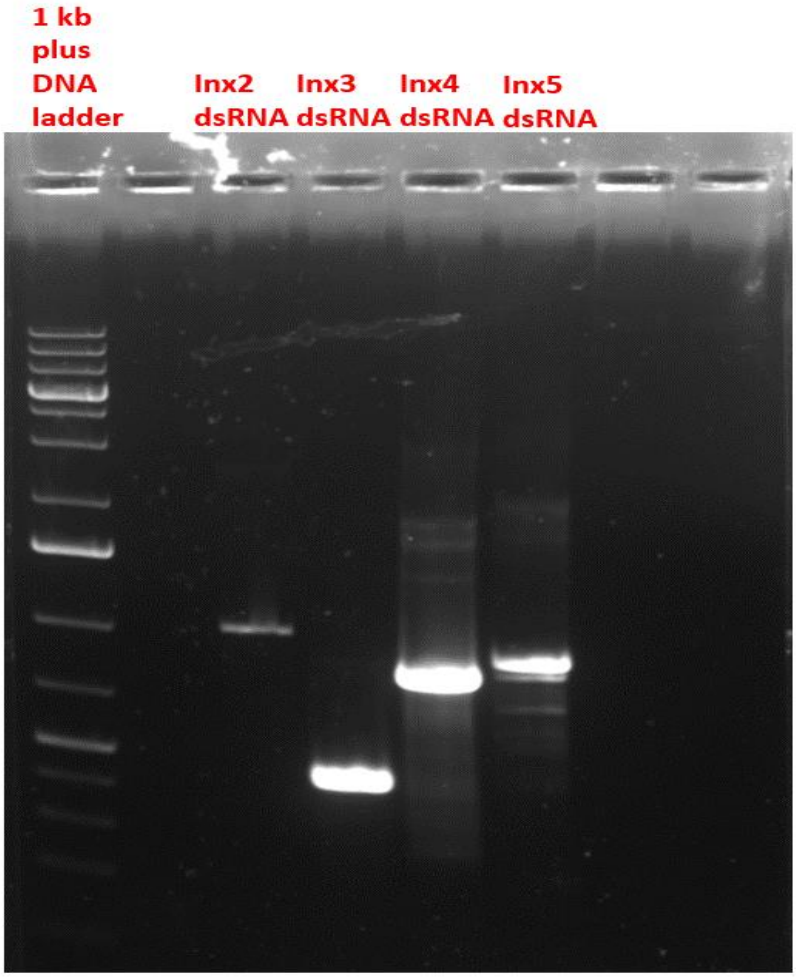

Lane 1 - 1kb plus DNA ladder. Lane 3 - Inx2 dsRNA (999 bp). Lane 4 - Inx3 dsRNA (320 bp).

Lane 5 - Inx4 dsRNA (796 bp). Lane 6 - Inx5 dsRNA (880 bp).

Figure 3

Crayfish behavior box.

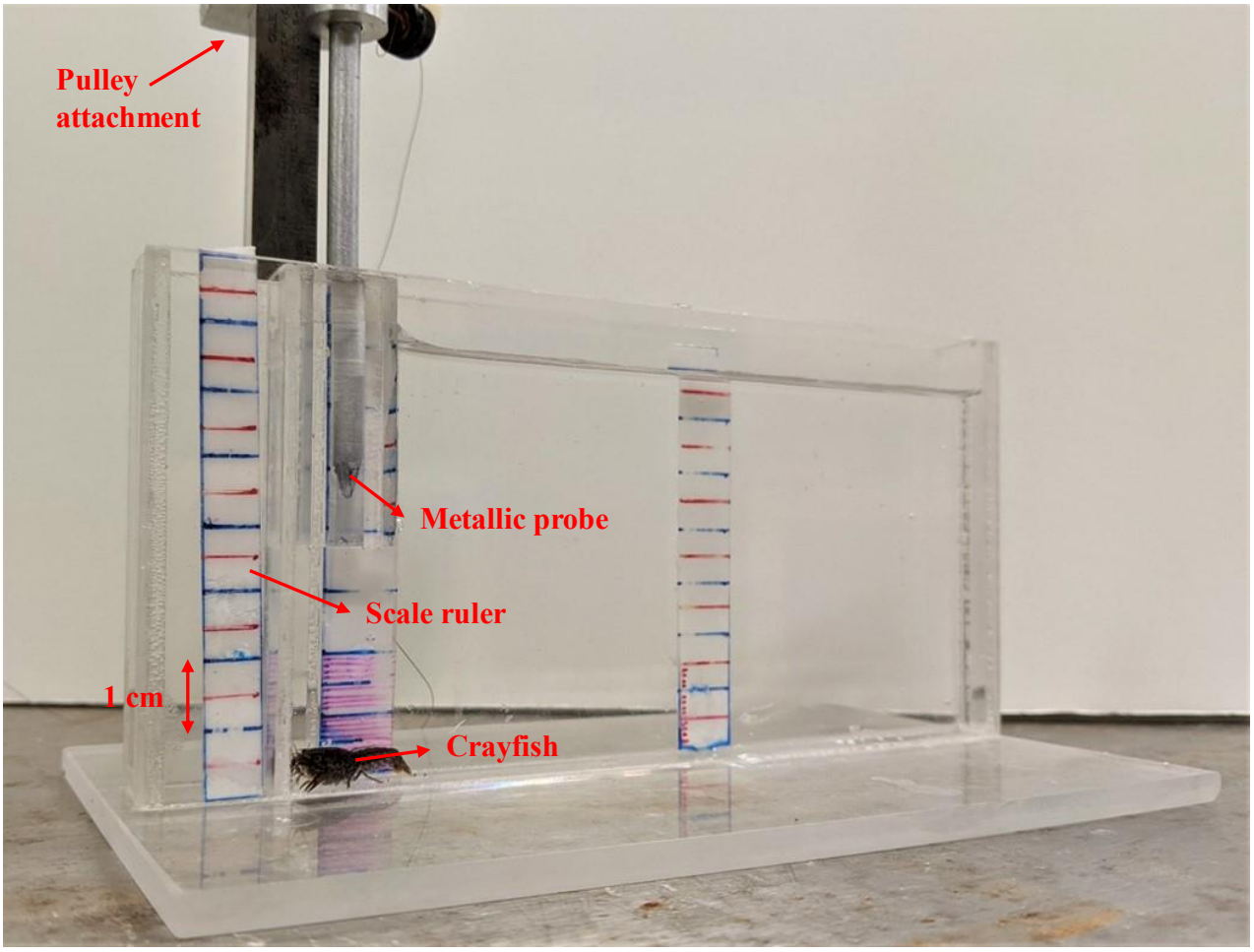

The animal is stimulated with a metallic probe either to the head (for MG tail-flip) or to the abdomen (for LG tail-flip). The probe is attached to a pulley that can be controlled by the experimenter. Markings are used for scaling purposes.

CHAPTER III: RESULTS

I. Identification of neuronal innexins in marbled crayfish

The marbled crayfish genome contains five putative innexin sequences

To identify putative innexin sequences in marbled crayfish, I used the published genome assembly of *P. virginalis* [Lyko et al, 2018] to find homologs of Drosophila innexins. I identified five different innexin sequences in the marbled crayfish genome using the NCBI BLAST server. Three of the identified innexins (hereafter referred to as Inx1, Inx2, and Inx3) showed significant homology with Drosophila innexin 2 while the other two (Inx4 and Inx5) showed high homology with Drosophila innexin 3. Moreover, marbled crayfish Inx3 also showed some homology with Drosophila ShakB innexin with a max score of 99.1 and e-value of 8e-67 [Table 2].

A multi-database search for conserved motifs resulted in the identification of pannexin and innexin motifs on all five crayfish innexins. Pannexins are the vertebrate homolog of invertebrate innexin proteins and hence share some sequence similarity [Baranova et al., 2004]. Moreover, all five putative crayfish innexins contained transmembrane domains, which are structural hallmarks of other innexin proteins [Phelan et al, 1998; Fig. 4]. Finally, invertebrate gap junction proteins contain a conserved domain encoded by YYQWV amino acid sequence that is found in their second transmembrane domain [Yen and Saier, 2007]. The amino acid projection of innexin transcripts was generated using the Expasy translate tool from the Swiss Institute of Bioinformatics (https://web.expasy.org/translate/). Innexins 1-4 contained the same YYQWV amino acid sequence [Fig. 5], suggesting that they have a high degree of conservation with other known innexin proteins that are involved in gap junctions.

Inx2-5 are expressed in marbled crayfish neurons

Previous studies have indicated that rectifying electrical synapses can be formed by an asymmetric distribution of gap junction proteins on either side of the synapse (heterotypic synapses) [Phelan et al, 2008]. Many of the electrical synapses in the MG and LG tail-flip circuits are rectifying [Swierzbinski and Herberholtz, 2018], posing the question which innexins may contribute to the formation of rectifying synapses in these circuits. The MG tail-flip is triggered by mechanical stimuli to the head which activates the mechanosensory afferents that excite the MG neuron via a chemical synapse [Swierzbinski and Herberholtz, 2018; Fig. 6A]. The MG neuron excites the MoG via a rectifying electrical synapse. The MG cell body and dendrites are located in the brain, but MG's axon projects posteriorly to the abdominal ganglia [first five segments] where its axon terminals constitute the presynaptic sides of the MG-MoG electrical synapse. MoG cell bodies are found in each of first five abdominal ganglia, with the sixth ganglion having a pair of giant motor axons [Furshpan and Potter, 1959]. Fig. 6A shows an example electrical synapse between MG and MoG in the 3rd abdominal segment.

Similarly, in the LG tail flip circuit, the LG neuron is activated by mechanical stimuli. Here, mechanosensory afferents from the tail excite LG via an electrical synapse. LG's cell body and dendrites are found in the abdominal ganglion 6. LG sends a long axon to the two most caudal thoracic and three most rostral abdominal ganglia and excites the MoGs in each of these ganglia through a rectifying electrical synapse to trigger the LG tail-flip escape. Fig. 6A shows an LG-MoG synapse at the 3rd abdominal segment as an example. Thus, unlike MG neuron, LG has both, a pre- and a postsynaptic gap junction site: postsynaptic for the sensory neuron – LG synapse and presynaptic for the LG – MOG synapse.

Fig 6B shows a simplified circuit design of LG and MG escape with various synaptic connections.

To identify which innexins may be present in the LG and MG circuits, I used PCR (Polymerase Chain Reaction) and agarose gel electrophoresis to test for expression of the various innexins in the brain and ventral nerve cord (composed of thoracic and abdominal ganglion) of marbled crayfish. Based on the synaptic architecture described above, I predicted that innexins involved in the presynaptic side of MG-MoG synapse will be expressed in the brain, while those involved in the postsynaptic side will be expressed in the ventral nerve cord. On the other hand, for the mechanosensory afferent-LG and LG-MoG synapse, both the pre- and post-synaptic innexins will show expression in ventral nerve cord.

To detect the expression of putative innexin genes in marbled crayfish nervous tissue, intron-spanning primers were designed to amplify specific innexin sequences from genomic DNA and cDNA from different tissue samples, following a previously described protocol [Abbi Benson, 2020]. I found that except Inx1, all four putative innexins showed significant expression in neuronal tissue [Fig. 7]. Inx2, 3, and 5 were expressed in the brain while Inx2, 3, 4, and 5 were expressed in the ventral nerve cord [Fig. 8]. Additionally, Inx2, 3, and 4 were expressed in abdominal flexor muscles [Fig. 8].

This indicated that innexins 2-5 may be involved in the formation of gap junction channels in the MG and LG circuits. Specifically, Inx2, 3, or 5 could constitute the presynaptic component of the rectifying MG to MoG synapse, and a nonmatching innexin (2,3,4 or 5) could provide the postsynaptic components, For the LG electrical synapses, all heterotypic combination of Inx2,3,4

and 5 are possible. Hence, Inx 2-5 were identified as candidate genes for RNAi to assess their contribution to the tail-flip escape behavior.

II. Identification of innexins involved in the crayfish escape circuit

Marbled crayfish contains the cellular machinery for RNAi

For the identification of innexins involved in crayfish tail-flip escape, I used RNA interference (RNAi) to knockdown specific innexin genes in marbled crayfish. Then, the contribution of individual innexins to the tail-flip circuit was studied using a reverse genetics approach by measuring the tail-flip behavior after each knockdown. For RNAi to work, the host organism must express DICER and ARGONAUTE proteins which are essential for different steps in the RNAi pathway [Wilson and Doudna, 2013]. Previous studies from the lab showed that marbled crayfish cells express the cellular machinery required for eliciting RNAi and that homologs of DICER and ARGONAUTE genes exist in crayfish [Abbi Benson, 2020]. The RNAi pathway begins with the cleavage of double stranded RNA (dsRNA) which is exogenously injected into the animal. This cleavage is mediated by the protein DICER and results in the formation of short RNA molecules known as silencing-induced RNA (siRNA). The siRNA then forms the RNAi induced silencing complex (RISC) after association with ARGONAUTE protein which binds to the target mRNA sequence to induce gene silencing [Wilson and Doudna, 2013; Fig 9]. To target individual innexin mRNA using the RNAi pathway, specific dsRNA needed to be designed to recognize and bind to the complementary mRNA sequence.

dsRNA was designed to target individual innexin sequences in marbled crayfish

Previous data have shown that dsRNA injection into juvenile crayfish resulted in a reduction of Inx2 expression 2 days after treatment [Abbi Benson, 2020]. The same study also provided initial evidence that this reduction in expression correlates with an increase in flexion and extension latencies for LG tail-flip. These experiments also provided the dsRNA to further test the impact of Inx2 on the MG tail-flip response. In addition, I designed dsRNA specific to Inx3, 4, and 5 using a kit method which utilizes a high-yield transcription reaction to synthesize duplex RNA strands from DNA template [MEGAscript RNAi kit, Thermo Fisher Scientific]. The DNA templates used for synthesis were verified by sequencing to ensure that the correct target sequence is being used [Table 3]. The resulting dsRNA molecules were run on an agarose gel to verify the size of the expected product [Fig 3]. dsRNA targeting the Drosophila myogenic determination (Dmyd) gene was used as control injection [Abbi Benson, 2020].

Silencing of Inx2 has no significant effect on MG tail-flip

The MG tail-flip was stimulated by using a metallic probe that hit the crayfish head within a rectangular animal cage [See Experimental Approach]. The tail-flip behavior was recorded using a high-speed camera [Yi Action Camera, Bellevue, WA, USA, 240 frames per second]. Behavior analysis was performed in Tracker software from Open-source physics [Brown, 2008]. Specifically, I measured the latency of the tail flexion and the time to peak velocity of tail-flip behavior for each animal tested, both before and after treatment with control/RNAi injections. Latency was measured as the delay between stimulus onset, i.e., the time of probe impact, and first complete flexion and was calculated as a product of the number of frames elapsed and frame duration. Tail-flip behavior assay was performed both before RNAi treatment (pre-treatment)

and 2 days after RNAi (post-treatment) and the behavioral data was compared between the two conditions. There was no significant change in latency 2 days after RNAi treatment in animals treated with Inx2 dsRNA (Paired t-test, p=0.35) [Fig 10]. In addition, there was no significant change in time to peak velocity after RNAi treatment in the same animals, suggesting that Inx2 silencing did not influence the overall speed of tail-flexion.

Inx3 silencing increases flexion latency for LG tail-flip but not for MG tail-flip

The LG tail-flip was stimulated with a metallic probe to the abdomen region which propels the animal in a jackknife reflex up and away from the stimulus. Behavioral recording and analysis were performed as stated earlier. As before, flexion latency was measured as the time difference between stimulus onset and the first full flexion during tail-flip. Behavioral data was compared between pre-treatment and post-treatment as stated in previous section. A significant increase in flexion latency was observed 2 days after treatment with Inx3 dsRNA (Paired t-test, p=0.007) [Fig 11]. No significant effect was found in animals treated with control dsRNA (p=0.2). The time to reach peak velocity remained unaffected by RNAi.

Similar experiments were performed to test the effect of Inx3 silencing on MG tail-flip. MG tail-flip was stimulated by a metallic probe to the head as previously described and tail-flip behavior was recorded before and 2 days after RNAi treatment. As before, the behavioral data was compared between pre-treatment (before RNAi) and post-treatment (2 days after RNAi) conditions for the same animal. There was no significant change in latency for the MG tail-flip post-treatment in animals treated with Inx3 dsRNA (Paired t-test, p=0.5) [Fig 12]. The time to peak velocity for the MG tail-flip was not affected by RNAi treatment.

Table 3

Alignment between putative innexins in marbled crayfish and the homologous fly innexins.

Marbled crayfish innexin	Drosophila innexin	Max alignment score	E-value
Innexin 1	Innexin 2	286	3e-118
Innexin 2	Innexin 2	350	6e-167
Innexin 3	Innexin 2	318	4e-90
Innexin 4	Innexin 3	124	2e-51
Innexin 5	Innexin 3	57	2e-11
Innexin 3	ShakB	99.1	8e-67

Marbled crayfish innexin transcripts were compared with the transcript sequence of Drosophila innexins using NCBI's BLAST tool. Maximum alignment scores >50 and e-values close to 0 were considered significant.

Figure 4

Motif and domain prediction for marbled crayfish innexins.

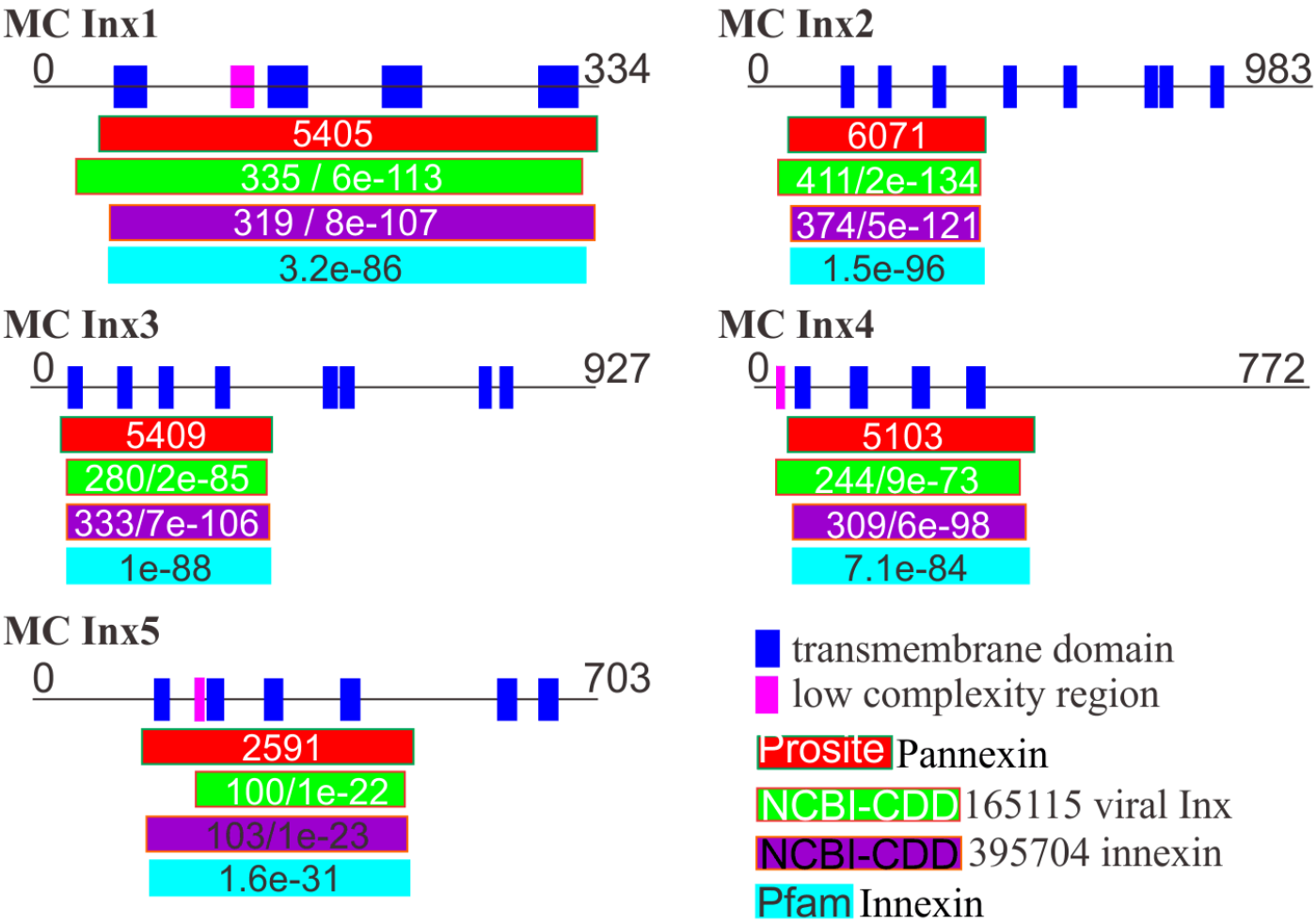

Predicted transmembrane domains are indicated by blue colored rectangular bars overlapping a continuous black line representing the span of the projected amino acid sequence for the respective innexin. Colored bars below the innexin sequence indicate alignment with pannexin and innexin motifs obtained from various sequence databases with the score and e-value given inside the bars.

Figure 5

Amino acid projection of marbled crayfish innexin aligned with a domain model of known innexin proteins for each of the five identified innexins in marbled crayfish.

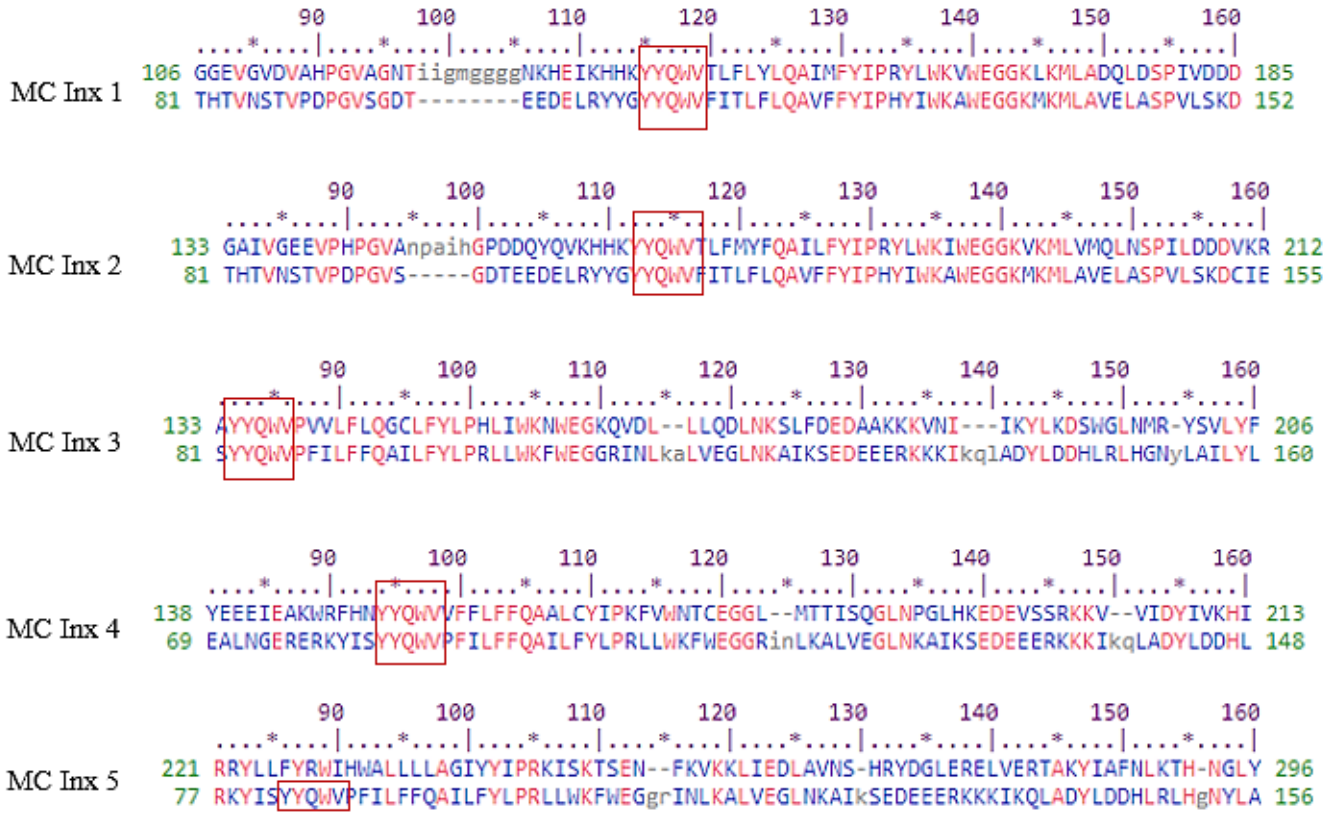

Top trace is amino acid projection of marbled crayfish innexin and bottom trace is the domain model of known innexin proteins. Marbled crayfish innexins 1-4 contain the conserved pentapeptide YYQWV shared among other known innexins.

Figure 6

A schematic of the MG and LG tail-flip circuit.

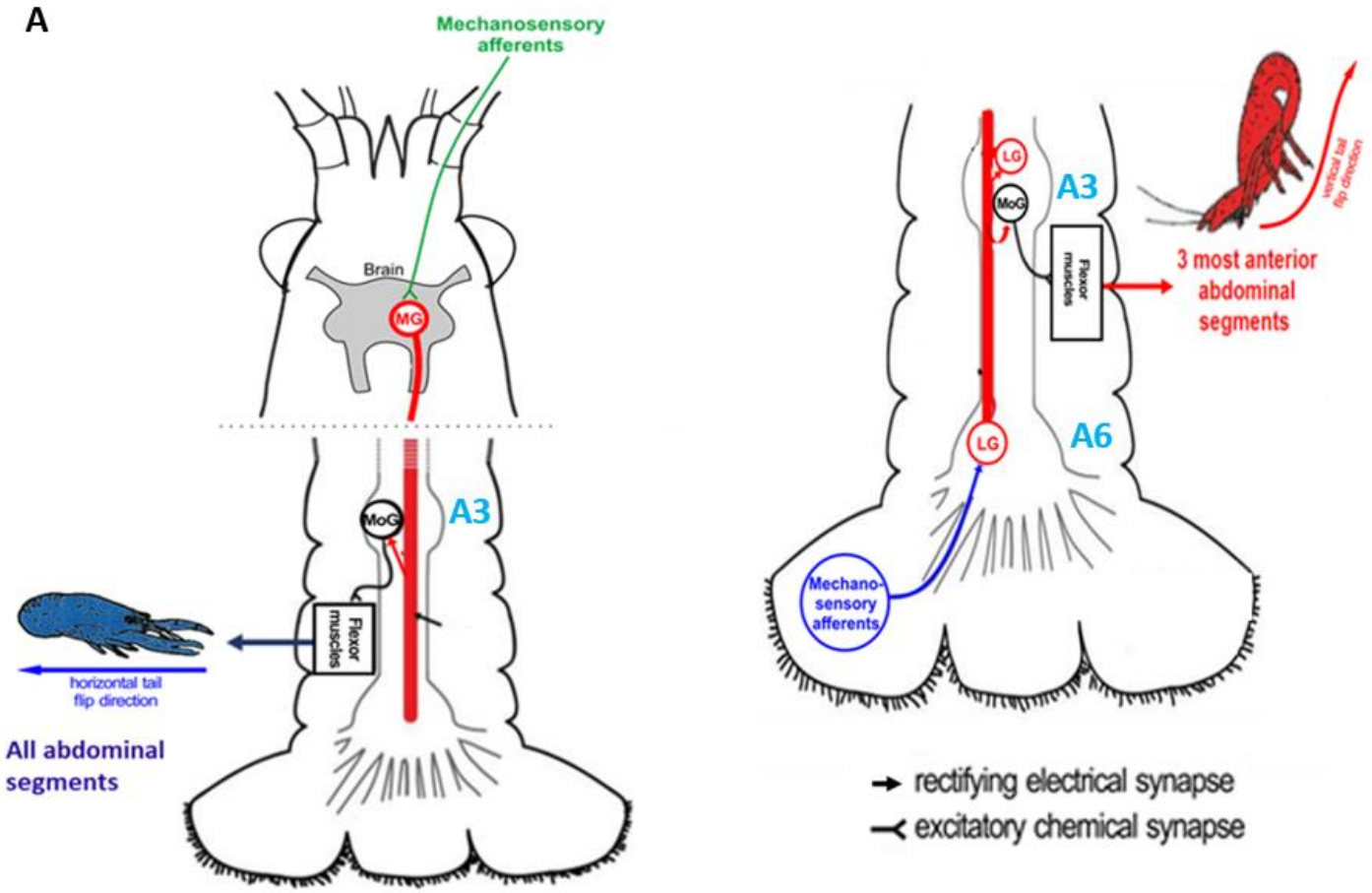

(Figure continues)

(Figure continued)

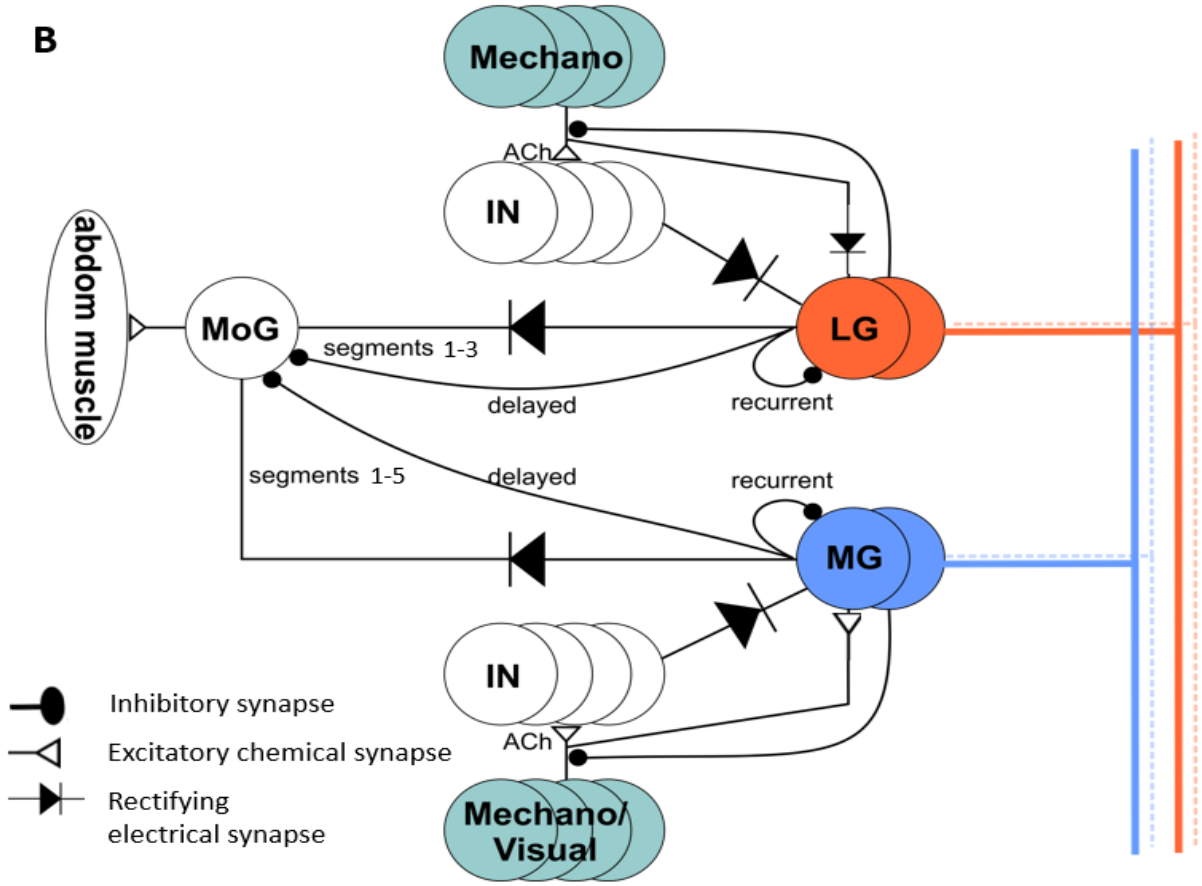

A. Rectifying electrical synapses and chemical synapses are indicated by distinct symbols as indexed in figure [Swierzbinski and Herberholz, 2018; Vu et al, 1997]. MG circuit is suggested to contain one rectifying electrical synapse between MG and MoG . The LG circuit contains two rectifying synapses – one between the mechanosensory afferents and LG, and another between LG and MoG . Both LG and MG trigger flexor muscle activation via MoG through an electrical synapse.

B. Simplified circuit diagram of LG and MG escape circuits showing the different connectivity patterns. Mechanosensory afferents excite LG via interneurons (indicated by IN) through cholinergic chemical synapses and rectifying electrical synapses, in addition to direct electrical synapses from the afferents. LG excites MoG in abdominal segments 1 through 3. MoG then excites the abdominal muscles that elicit the tail flip ("abdom muscle in figure"). Delayed inhibitory synapses prevent the continuous excitation of command neurons and motor neurons after the tail flip. MG is excited by mechanosensory and visual afferents, directly through chemical synapses and indirectly via interneurons through chemical and rectifying electrical synapses. MG excites MoG in abdominal segments 1-5.

Figure 7

Gel electrophoresis image of marbled crayfish innexin sequences amplified from neuronal and muscle mRNA using PCR.

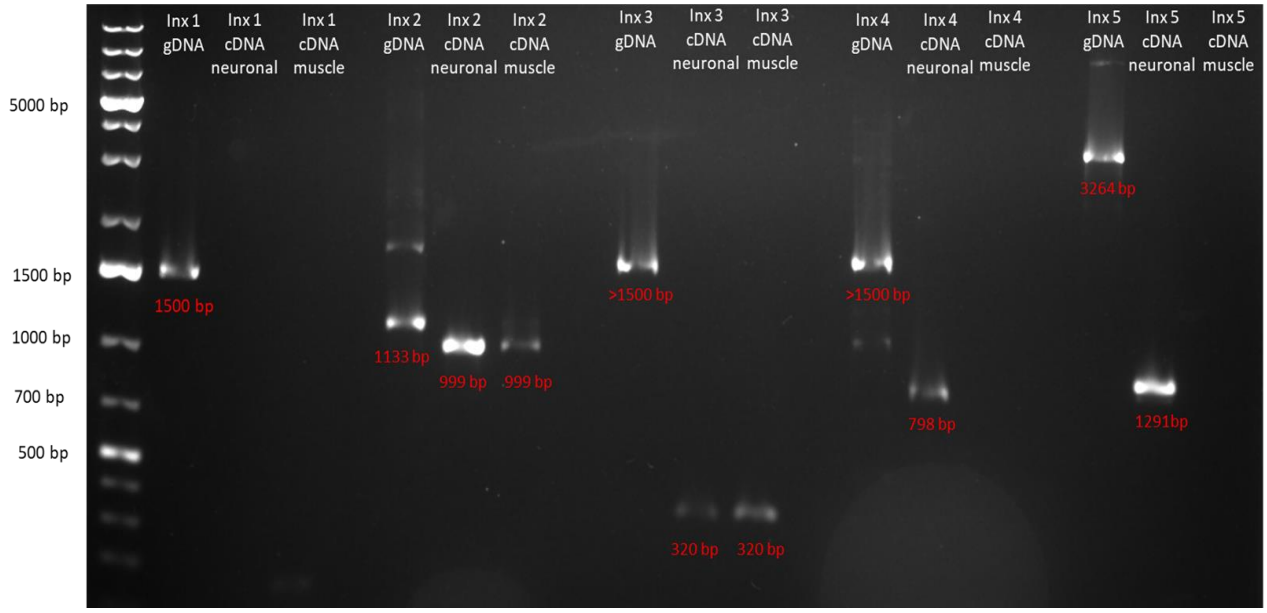

The first lane contains 1kb plus DNA ladder, with sequence length indicated on the left. mRNA was extracted from neuronal (brain and whole ventral nerve cord) and muscle tissue and converted to cDNA. Template cDNA was PCR amplified with specific innexin primer (intron spanning). Expected product sizes are indicated underneath each gel band.

Figure 8

Gel electrophoresis image of marbled crayfish innexin sequences amplified from brain and whole ventral nerve cord mRNA separately using PCR.

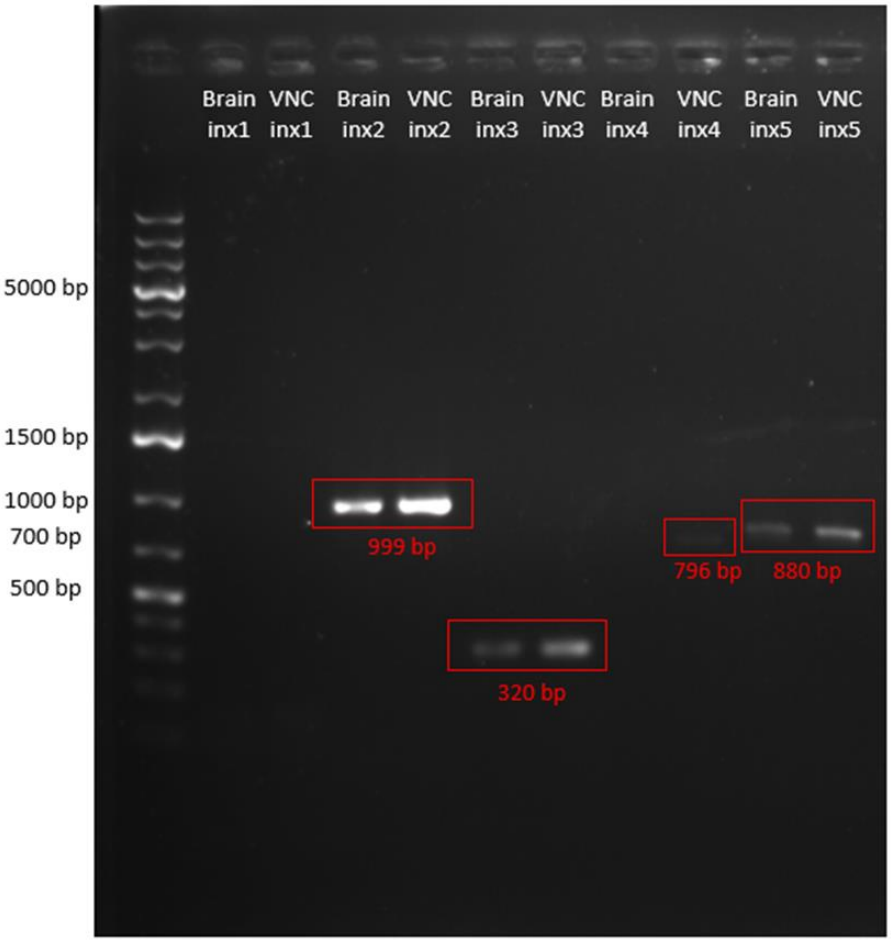

The first lane contains 1kb plus DNA ladder. mRNA was extracted from brain and whole ventral nerve cord and converted to cDNA. Template cDNA was PCR amplified with specific innexin primer. Expected product sizes are indicated underneath each gel band.

Figure 9

Mechanism of RNA interference to acutely reduce innexin expression.

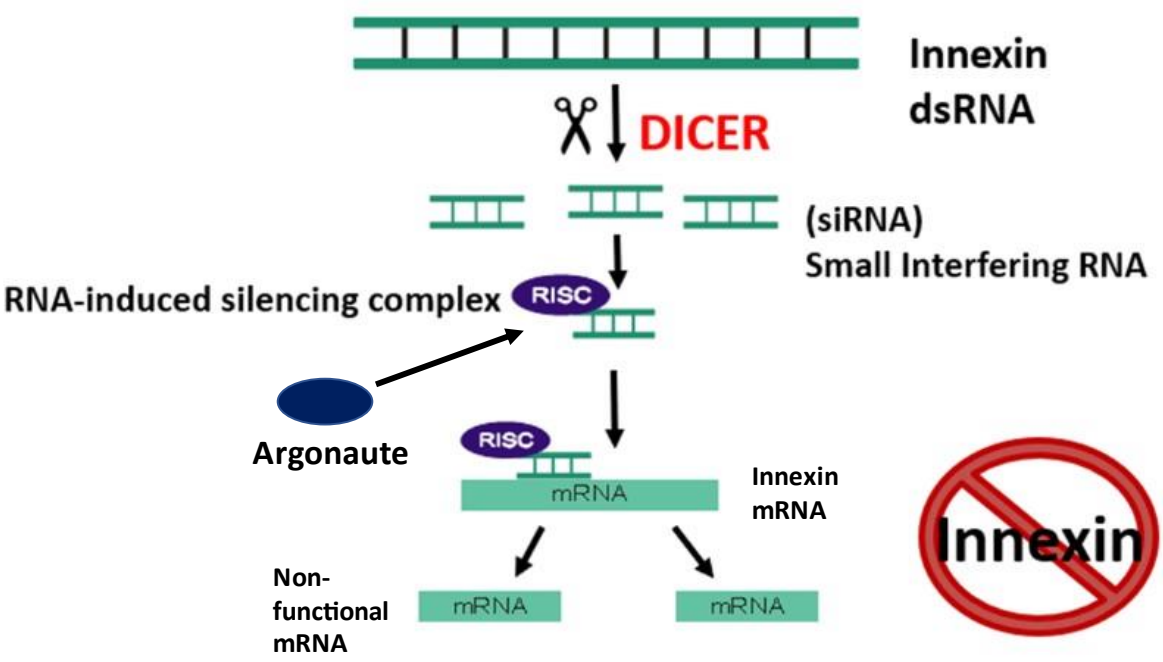

Inx dsRNA is injected into the animal to temporarily reduce the expression of targeted innexin gene via mRNA degradation. The injected dsRNA is broken down into siRNA (small interfering RNA) molecules by the DICER protein in the cell. Then, another protein called Argonaute forms a complex with the siRNA molecule to generate RISC (RNA Induced Silencing Complex). RISC binds to the corresponding mRNA molecule and breaks it down to small non-functional pieces, thus effectively knocking down gene expression.

Table 4

Sequence alignment generated using NCBI's BLAST server.

Query	Subject	Max score	E-value
Inx 2 FP sequence	TR 16976	480	3e-139
Inx 2 RP sequence	TR 16976	1165	0
Inx 3 FP sequence	TR 20134	478	2e-138
Inx3 RP sequence	TR 20134	297	6e-84
Inx5 FP sequence	TR 6064	1108	0
Inx5 RP sequence	TR 6064	1233	0

Sequencing reads for each innexin DNA used as template for dsRNA synthesis was taken as query while the transcript sequence for that specific innexin was taken as the subject sequence in the blast tool. Sequencing reads were generated using both forward and reverse primers.

Figure 10

Change in flexion latency of MG tail-flip after RNAi treatment for control and treatment groups (Inx2).

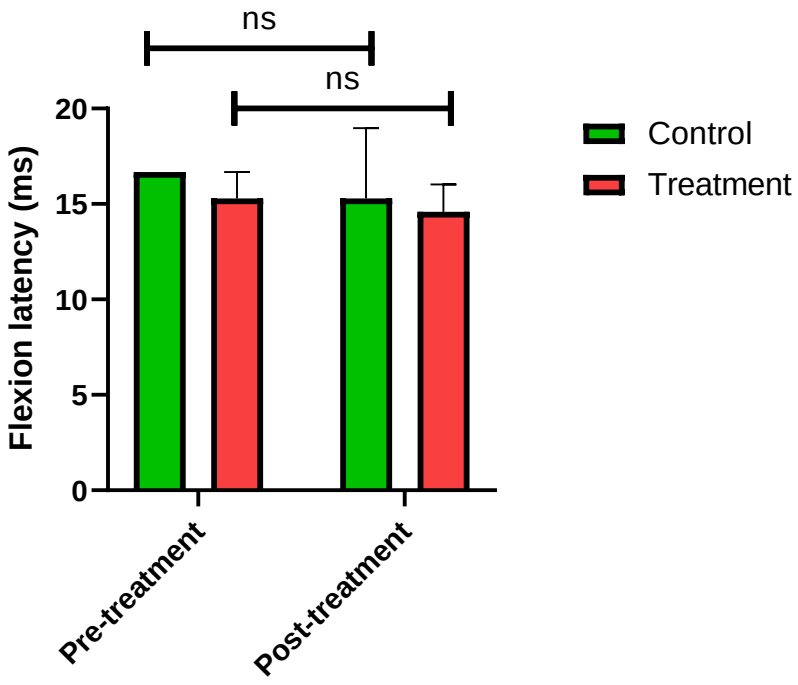

Control animals were injected with sham dsRNA while animals in the treatment group were injected with Inx2 dsRNA. Post-treatment behavior testing was done 48 hours after injection. N for control = 3, N for treatment = 6. Significance testing was done using paired t-test, 1 tailed distribution. Significance was assumed at $\alpha = 0.05$.

Figure 11

Change in flexion latency of LG tail-flip after RNAi treatment for control and treatment groups (Inx3).

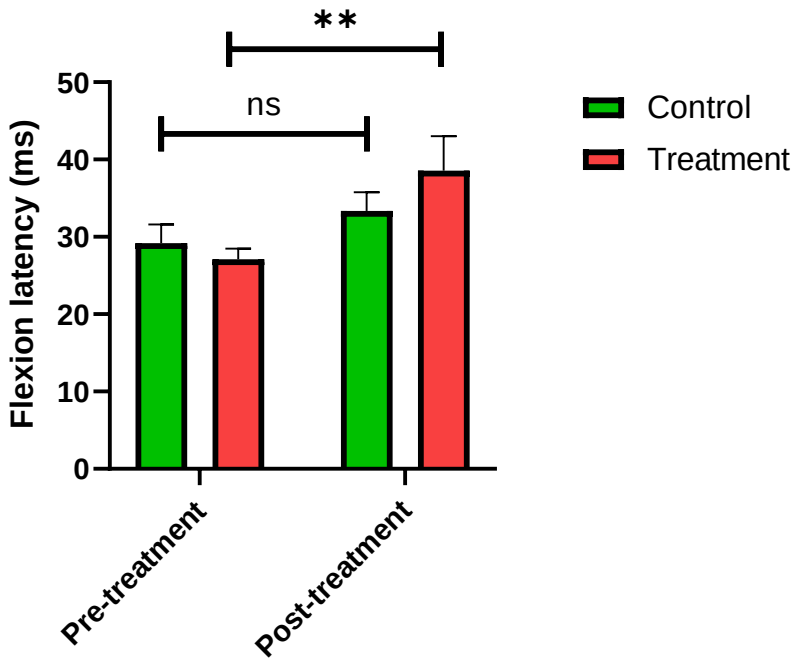

Control animals were injected with sham dsRNA while animals in the treatment group were injected with Inx3 dsRNA. Post-treatment behavior testing was done 48 hours after injection. N for control = 4, N for treatment = 8. Significance testing was done using paired t-test, 1 tailed distribution. **p<0.01.

Figure 12

Change in flexion latency of MG tail-flip after RNAi treatment for control and treatment groups (Inx3).

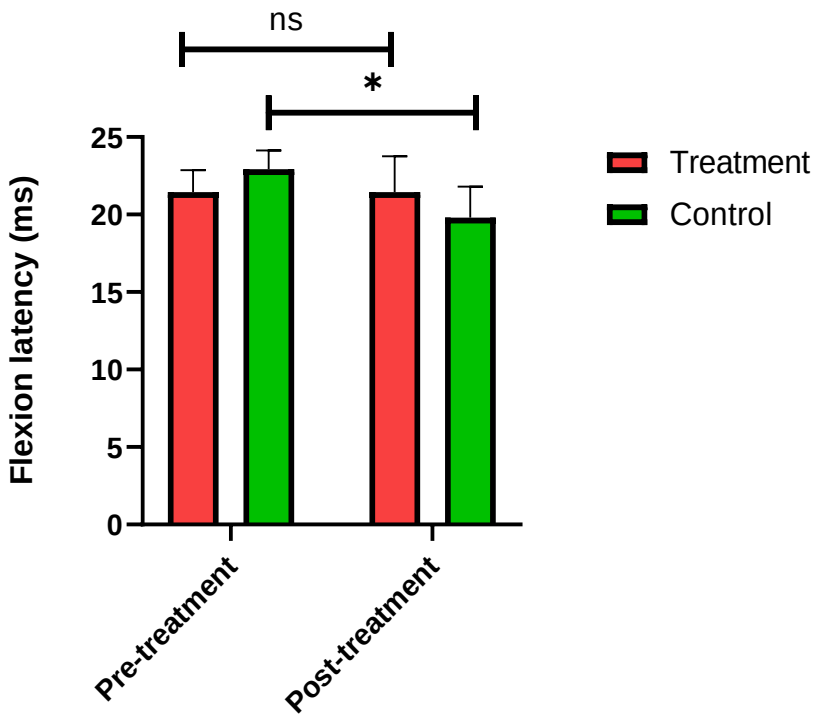

Control animals were injected with sham dsRNA while animals in the treatment group were injected with Inx3 dsRNA. Post-treatment behavior testing was done 48 hours after injection. N for control = 4, N for treatment = 7. Significance testing was done using paired t-test, 1 tailed distribution. *$p<0.05$.

CHAPTER IV: DISCUSSION

Although the crayfish escape response has been widely studied due to its easy access and well-characterized neural circuitry [Edwards et al., 1999]], the molecular underpinning of the tail-flip escape circuit is still not fully understood. Specifically, the gap junction proteins that contribute to the formation of electrical synapses in the escape circuit remain largely elusive. Using comparative genomics, I was able to identify five putative innexins in the marbled crayfish genome based on homology with known innexin sequences, particularly Drosophila innexins. These innexins share many of the structural properties of other known innexin proteins which make them adept to function in gap junction channels, e.g., the presence of multiple transmembrane domains that can form a bridge between adjacent cells. Also, four of the five identified innexins had the conserved YYQWV motif in their amino acid sequence suggesting a strong similarity with most of the known innexin proteins. Inx5 did not share this signature motif which may be a result of a gene duplication event leading to molecular evolution. Thus, Inx5 might be functionally distinct from other crayfish innexins, however its role in gap junction channels cannot be eliminated based solely on amino acid variations in a single motif. Four of the five innexins showed significant expression in neuronal tissue, suggesting their possible role in crayfish neurophysiology, viz-a-viz the formation of gap junction channels between neurons. To test the role of these innexins in the escape circuit, I used a reverse genetics approach using RNAi silencing of innexin genes to assess the effects of gene knockdown on behavior.

Heterotypic distribution of gap junction proteins favors rectification at the synapse

It has been suggested that rectification is achieved by asymmetric distribution of gap junction proteins on either side of the synapse. This asymmetry in hexamer composition on the pre- and post-synaptic side results in differential voltage-dependent gating and conductance at the synapse, thus biasing current flow in one direction over the other [Harris, 2002]. Thus, it can be assumed that innexin proteins with appreciably different characteristics will result in rectification when arranged asymmetrically at the synapse. Consequently, multiple different combinations of identified innexins in crayfish may lead to rectification at the electrical synapse in the escape circuit. However, their specific arrangement in the hexamers and in the heterotypic assembly cannot be effectively predicted by this study, apart from the observation that three of them showed expression in the brain and the ventral nerve cord, suggesting that these may be present on the presynaptic side of the MG circuit. Nonetheless, silencing these innexins is expected to result in a lack of robust signal transmission between neurons, given that they may be essential to the formation of gap junctions.

RNAi silencing of innexins may disrupt gap junction channels and increase synaptic delay

Since electrical synapses in the LG and MG escape circuits are made up of gap junctions, and these gap junctions are known to be formed by innexin proteins in invertebrates, I hypothesized that the homologs of invertebrate innexin proteins in crayfish are responsible for the formation of electrical synapses in the escape circuit. There was a significant reduction in expression of innexins in marbled crayfish 2 days after treatment with innexin dsRNA. The half-life of innexin proteins has been found to be fairly short, in the order of a few hours [Curtin et al., 2002]. Thus, an acute knockdown of innexin expression in the cells will essentially result in disruption of gap

junction formation and turnover, which will only be rescued once the expression of the silenced innexin protein returns to normal levels after the injected dsRNA has been degraded. Therefore, it is expected that within this time window of innexin downregulation, gap junctions present between the command neurons and the motor neurons (for both MG and LG circuit) and between the mechanosensory afferents and command neurons (in case of LG circuit) may be compromised. This, in turn, will lead to less efficient transmission of electrical signals between these neurons and hence the tail-flip behavior will suffer a delay, as was seen in LG escape after silencing of Inx2 and Inx3. This delay in behavior may be attributed to an increase in synaptic delay caused by the disruption of gap junctions present at the synapse. Downregulation of an innexin gene will lead to reduction in the number of gap junction channels made up of that specific innexin, and hence lower the synaptic conductance. This, in turn, will result in greater synaptic delay because the postsynaptic buildup of excitation is slower and action potential threshold will be reached more slowly. The increased synaptic delay will consequently increase the delay in response onset, as was seen in the tail-flip behavior. The absence of an effect for MG tail-flip after RNAi seems to suggest that the change in electrical transmission at an individual synapse is insufficient to elicit a detectable behavioral deficit and it is only when two electrical synapses (as is the case with LG circuit) are disrupted together that the behavioral deficit becomes obvious. Additionally, spatial summation at the rectifying electrical synapses between mechanosensory afferents and LG is likely reduced following innexin knockdown because of the reduced synaptic conductance. This will result in an additional delay in synaptic transmission across the LG circuit. On the other hand, MG neuron receives sensory inputs via chemical synapses, which are not affected by innexin knockdown. Any delay in synaptic transmission will thus be restricted to the postsynaptic MG-MoG synapse. Nonetheless, the effects of silencing of

one innexin in an individual synapse may be compensated for by upregulated expression of other innexin protein (s) which may be involved in forming that gap junction. Thus, it would be interesting to look at the expression levels of other identified innexins in crayfish following RNAi of one innexin protein to investigate a possible compensatory mechanism for gap junction formation in synapses that mediate a behavior as vital as the tail-flip escape. Furthermore, it will be important to look at the effect of innexin silencing on the rectification property of these synapses and try to relate that to the change in behavioral response. However, any speculations about how rectification might be implicated in the effects seen in this study remain unyielding in the absence of electrophysiological data.

Gap junctions in MG and LG escape circuit may be constitutively different

The MG cell body is present in the brain while the LG cell body is localized in the sixth abdominal ganglion. MoG neurons also have their cell bodies in each of the first five abdominal ganglion [Edwards, 2017]. Hence, it is expected that innexins involved in the LG escape circuit will be expressed in the abdominal ganglia since the LG-MoG synapse is formed in the caudal thoracic and rostral abdominal ganglia with the cell bodies of both the presynaptic and postsynaptic neurons present in the abdominal segments, as stated above. The soma of the MG neuron is in the brain [Edwards, 2017], hence it is expected that innexins forming the presynaptic side of MG-MoG synapse will have expression in the brain tissue while those in the post-synaptic side will be expressed in the first five abdominal ganglion. Using gene amplification and gel electrophoresis, I found that Inx2, 3, and 4 are expressed in the brain while Inx2, 3, 4, and 5 are expressed in the abdominal ganglia. In previous studies, Inx2 silencing was shown to have detrimental effects on the LG tail-flip in marbled crayfish [Abbi Benson, 2020]. Hence, I

conducted experiments to test the effects of Inx2 silencing on the MG tail-flip, since both these circuits involve rectifying synapses between the giant command neuron (LG/MG) and motor neuron, and it is possible that the same innexin protein(s) might mediate synaptic transmission in both the circuits. The same approach of RNAi silencing followed by escape behavior assay was used to study the effects of silencing of other innexin genes in crayfish. My research showed that at least two of the five identified innexins, i.e., Inx2 and Inx3, may be involved in the formation of electrical synapses in the LG escape circuit since their knockdown disrupts the escape response associated with the LG command neurons. On the contrary, silencing the same two innexins did not influence the MG escape response, suggesting that the MG escape circuit, mediated by the MG neurons, could depend on innexin proteins other than Inx2 and Inx3. From these results, it can be concluded that Inx2 and Inx3 may be involved in the formation of electrical synapses between mechanosensory afferents and the LG neuron and/or between LG neuron and the motor neuron, but not in the MG circuit. This difference in the constitution of gap junctions in the two forms of escape circuit may be consistent with the fact that LG and MG escape circuits may have evolved differently over time to elicit the two distinct types of escape [Krasne, Heitler, and Edwards, 2014 (book chapter)], hence the molecular composition of these circuits might also be variable. Nonetheless, the absence of an effect of innexin silencing on MG tail-flip might not necessarily imply the absence of these innexin proteins in the MG tail-flip circuit. The MG circuit has only one rectifying synapse present between the medial giant neuron and the motor giant neuron [Edwards, 2017], unlike the LG circuit which has at least two rectifying synapses. Thus, it is possible that silencing one of the innexin proteins in the MG circuit may not have a detectable effect on the overall speed of signal transmission as reflected in the response latency.

My assumption is that the latency of flexion, i.e., time delay between the onset of stimulus and the first complete flexion of the abdomen, will be a function of the speed of signal transmission between the mechanosensory afferents to the flexor muscles. In the case of MG response, this pathway would involve a chemical synapse between mechanosensory afferent and MG neuron, one electrical synapse between MG neuron and motor neuron, and another chemical synapse between motor neuron and flexor muscles. On the other hand, the LG response would involve two electrical synapses – one between the mechanosensory afferent and the LG neurons and one between LG neuron and motor neuron, and one chemical synapse between motor neuron and flexor muscle. Thus, silencing of only one innexin gene in either of the circuits may have differential effects on behavior depending on which (if any) of the gap junction channels in the circuit is compromised. A temporary knockdown of one of the innexin proteins in a heterotypic channel might not be sufficient to induce a significant behavioral deficit unless the effect is duplicated in more than one gap junction channel (as may be the case in the LG circuit). It is likely that the molecular constitution of a rectifying synapse in the escape circuit is highly flexible given its importance for survival of the organism and a one-off silencing of an innexin protein might be compensated by another innexin protein at the synapse. Hence, it would be interesting to study the effects of silencing of multiple innexin genes at once on the tail-flip behavior.

REFERENCES

1. Auerbach, A. A., & Bennett, M. V. L. (1969). A rectifying electrotonic synapse in the central nervous system of a vertebrate. *Journal of General Physiology*, *53*(2), 211–237. https://doi.org/10.1085/jgp.53.2.211
2. Baranova, A., Ivanov, D., Petrash, N., Pestova, A., Skoblov, M., Kelmanson, I., Shagin, D., Nazarenko, S., Geraymovych, E., Litvin, O., Tiunova, A., Born, T. L., Usman, N., Staroverov, D., Lukyanov, S., & Panchin, Y. (2004). The mammalian pannexin family is homologous to the invertebrate innexin gap junction proteins. *Genomics*, 83(4), 706–716. https://doi.org/10.1016/j.ygeno.2003.09.025
3. Benson, A. (2020). Identification of innexins contributing to giant-fiber escape responses in marbled crayfish.
4. Curtin, K. D., Zhang, Z., & Wyman, R. J. (2002). Gap Junction Proteins Expressed during Development Are Required for Adult Neural Function in the Drosophila Optic Lamina. The Journal of Neuroscience, 22(16), 7088–7096. https://doi.org/10.1523/JNEUROSCI.22-16-07088.2002
5. Derby, C., & Thiel, M. (Eds.). (2014). *Nervous systems and control of behavior*. Oxford University Press.
6. Edwards, D. (2017). Crayfish Escape. In *Oxford Research Encyclopedia of Neuroscience*. https://doi.org/10.1093/acrefore/9780190264086.013.158

7. Edwards, D. H., Heitler, W. J., & Krasne, F. B. (1999). Fifty years of a command neuron: The neurobiology of escape behavior in the crayfish. *Trends in Neurosciences, 22*(4), 153–161. https://doi.org/10.1016/S0166-2236(98)01340-X
8. Furshpan, E. J., & Potter, D. D. (1959). Transmission at the giant motor synapses of the crayfish. *The Journal of Physiology*, *145*(2), 289–325. https://doi.org/10.1113/jphysiol.1959.sp006143
9. Giaume, C., Kado, R. T., & Korn, H. (1987). Voltage-clamp analysis of a crayfish rectifying synapse. *The Journal of Physiology*, *386*(1), 91–112. https://doi.org/10.1113/jphysiol.1987.sp016524
10. Gutekunst, J., Andriantsoa, R., Falckenhayn, C., Hanna, K., Stein, W., Rasamy, J., & Lyko, F. (2018). Clonal genome evolution and rapid invasive spread of the marbled crayfish. *Nature Ecology & Evolution*, *2*(3), 567–573. https://doi.org/10.1038/s41559-018-0467-9
11. Harris, A. L. (2002). Voltage-sensing and Substate Rectification. Journal of General Physiology, 119(2), 165–170. https://doi.org/10.1085/jgp.119.2.165
12. Marder, E. (1998). Electrical synapses: Beyond speed and synchrony to computation. *Current Biology*, *8*(22), R795–R797. https://doi.org/10.1016/S0960-9822(07)00502-7
13. Marder, E., & Calabrese, R. L. (1996). Principles of rhythmic motor pattern generation. *Physiological Reviews*, *76*(3), 687–717. https://doi.org/10.1152/physrev.1996.76.3.687
14. Phelan, P., Bacon, J. P., A. Davies, J., Stebbings, L. A., & Todman, M. G. (1998). Innexins: A family of invertebrate gap-junction proteins. *Trends in Genetics*, *14*(9), 348–349. https://doi.org/10.1016/S0168-9525(98)01547-9

15. Phelan, P., Goulding, L. A., Tam, J. L. Y., Allen, M. J., Dawber, R. J., Davies, J. A., & Bacon, J. P. (2008). Molecular mechanism of rectification at identified electrical synapses in the drosophila giant fiber system. *Current Biology*, *18*(24), 1955–1960. https://doi.org/10.1016/j.cub.2008.10.067
16. Rela, L., & Szczupak, L. (2004). Gap junctions: Their importance for the dynamics of neural circuits. *Molecular Neurobiology*, *30*(3), 341–358. https://doi.org/10.1385/MN:30:3:341
17. Santer, R. D., Yamawaki, Y., Rind, F. C., & Simmons, P. J. (2008). Preparing for escape: An examination of the role of the DCMD neuron in locust escape jumps. *Journal of Comparative Physiology A*, *194*(1), 69–77. https://doi.org/10.1007/s00359-007-0289-8
18. Stein, W., DeMaegd, M. L., Benson, A. M., Roy, R. S., & Vidal-Gadea, A. G. (2022). Combining Old and New Tricks: The Study of Genes, Neurons, and Behavior in Crayfish. *Frontiers in Physiology*, *13*, 947598. https://doi.org/10.3389/fphys.2022.947598
19. Swierzbinski, M. E., & Herberholz, J. (2018). Effects of ethanol on sensory inputs to the medial giant interneurons of crayfish. *Frontiers in Physiology*, *9*, 448. https://doi.org/10.3389/fphys.2018.00448
20. Tabor, K. M., Bergeron, S. A., Horstick, E. J., Jordan, D. C., Aho, V., Porkka-Heiskanen, T., Haspel, G., & Burgess, H. A. (2014). Direct activation of the Mauthner cell by electric field pulses drives ultrarapid escape responses. *Journal of Neurophysiology*, *112*(4), 834–844. https://doi.org/10.1152/jn.00228.2014
21. Wilson, R. C., & Doudna, J. A. (2013). Molecular mechanisms of rna interference. *Annual Review of Biophysics*, *42*(1), 217–239. https://doi.org/10.1146/annurev-biophys-083012-130404

22. Yen, M. R., & Saier, M. H. (2007). Gap junctional proteins of animals: The innexin/pannexin superfamily. *Progress in Biophysics and Molecular Biology*, *94*(1–2), 5–14. https://doi.org/10.1016/j.pbiomolbio.2007.03.006